RAA 2014 Vol. **14** No. **3**, 357–366 doi: 10.1088/1674–4527/14/3/009
http://www.raa-journal.org *http://www.iop.org/journals/raa*

***R**esearch in*
***A**stronomy and*
***A**strophysics*

Isospin violation in the d(n,γ)^{3}H process at energies relevant for big bang nucleosynthesis

Hossein Sadeghi, Hassan Khalili and Mojtaba Godarzi

Department of Physics, Faculty of Science, Arak University, Arak 38156-8-8349, Iran;
h-sadeghi@araku.ac.ir

Received 2013 February 28; accepted 2013 October 14

Abstract The cross section for a neutron-deuteron (nd) radiative capture is calculated using the pionless effective field theory including isospin symmetry breaking (ISB) corrections up to higher order. The triton is studied as a three-body bound state and one has to take into account various ISB effects, relativistic corrections and external electromagnetic currents. The isospin violation in nd radiative capture is improved compared to the one at NLO and N^{2}LO. The cross section is determined to be $\sigma_{\rm tot} = [0.505 \pm 0.003]$ mb up to N^{2}LO. A satisfactory agreement between theory and experiment for the calculated cross section has been found by insertion of three-body forces and ISB effects.

Key words: nuclear reactions — nucleosynthesis — kinematics and dynamics

1 INTRODUCTION

Isospin symmetry breaking (ISB) in nuclear force has been studied for a long time. The hadrons appear in isospin multiplets, characterized by very tiny splittings on the order of a few MeV. These are generated by the small mass difference in quarks ($m_{\rm u} - m_{\rm d}$) and electromagnetic effects of the same size (Marciano & Pagels 1978). The reason for the recent interest in ISB is the hope that a detailed understanding of it could tell something about the underlying structure of hadrons in terms of quarks (Iqbal & Niskanen 1988).

The study of a three-body nuclear system involving neutron radiative capture by a deuteron has been investigated in theoretical and experimental works over the past decades. The experimental result of this process has been measured by Jurney et al. (1982).

In theoretical investigation, this reaction was studied by employing Faddeev calculations with inclusion of three-body forces and pion exchange currents by Friar et al. (1990). More recently, a rather detailed investigation of such processes has been performed by Viviani et al. (Viviani et al. 1996; Marcucci et al. 1998). Their calculation is based on a modern nucleon-nucleon potential, Argonne V18 (AV18). This potential has 18 operators. Fourteen operators are charge independent, corresponding to an updated version of Argonne V14 (AV14). Three charge-dependent operators have been added due to the aspect of isospin breaking in the strong interaction and a one charge-asymmetric operator to explain the difference in the proton-proton and neutron-neutron scattering lengths. They obtained the cross section to be 0.600(0.578) (mb) for two nucleon interactions with AV18 (and three nucleon interactions with Urbana IX). Song et al. (2009) have reported values for the neutron-deuteron (nd) radiative capture cross section, by utilizing a meson exchange current derived up to N^3LO incorporating heavy baryon chiral perturbation theory (HBχPT). Recently, Girlanda et al. (2010) also studied the nd radiative captures at thermal neutron energies, using wave-functions obtained from either chiral or conventional two- and three-nucleon realistic potentials by implementing a method based on hyperspherical harmonics, and electromagnetic currents derived in chiral effective field theory (χEFT) up to one loop.

EFT is well suited for exploring the consequences of the ISB effect for low-energy dynamics of many-nucleon systems. Consider first the effect of strong isospin violation. The effects of isospin violation within an EFT framework have been developed over the past decade (van Kolck et al. 1998; Walzl et al. 2001; Friar et al. 2004; Epelbaum et al. 2005; Epelbaum & Meißner 2005). There is even further symmetry related to the quark mass term. One improvement is the inclusion of effects of isospin breaking due to differences in quark mass. One can see that isospin breaking would only have a small impact on these findings.

We have suggested a method for computation of nd radiative capture for extremely low energy with pionless EFT (Sadeghi & Bayegan 2005; Sadeghi et al. 2006; Sadeghi 2007, 2008; Sadeghi & Bayegan 2010), where with this formalism, we can estimate errors of a few percent in perturbative expansion up to N^2LO compared with the file of compiled nuclear data from the ENDF/B online database[1] and available experimental data. A variety of observables of the triton, cross sections as well as electric form factor have been calculated and compared with the corresponding experimental results at low energies.

The present study focuses on effects of isospin breaking in which different physical masses is incorporated. This approach allows for isospin corrections since the masses of the particles are taken to be different. The changes induced by the extra isospin violation are rather small compared with the errors that we have obtained.

This article is organized as follows. In the next section, a brief description of the relevant Lagrangian and nd scattering is reported. Then the formalism for total cross section of the nd radiative capture will be presented in Section 2. We discuss the theoretical errors, tabulation of variations in cut-off for the calculated cross section compared with other theoretical approaches and available experimental data in Section 3. Finally, a summary and conclusions follow in Section 4.

2 THE LAGRANGIAN FOR NUCLEON-DEUTERON INTERACTION AND CURRENTS

We will briefly review isospin breaking in the strong interaction and nuclear EFT without pions. We have decided to give an overview of the dominant ISB contributions up to higher orders. The QCD quark mass term is given by

$$\mathcal{L}_{\rm mass}^{\rm QCD} = -\frac{1}{2}\bar{q}\,(m_{\rm u} + m_{\rm d})(1 - \beta\tau_3)\,q\,, \tag{1}$$

where $\beta \equiv \frac{m_{\rm d}-m_{\rm u}}{m_{\rm d}+m_{\rm u}} \sim \frac{1}{3}$. The isoscalar term in Equation (1) leads to the nonvanishing pion mass and breaks chiral symmetry, $M_\pi^2 = (m_{\rm u} + m_{\rm d})B \neq 0$. (The constant B describes the strength of the bilinear light quark condensates.) We note that effects from isospin violation are much smaller than the numerical value of β (Epelbaum & Meißner 2005). Here, we will make use of the following simple counting rules which dominate ISB for short-range interactions where $\beta \sim e \sim \frac{Q}{\Lambda}$. In addition to the counting rules, there is the extra $1/(4\pi)^2$ factor, which arises from calculation of loop integrals. The above mentioned counting rules suggest a different counting of the strong interactions when the effects of isospin breaking are included (in comparison with Walzl et al. 2001).

[1] The ENDF/B online database is part of the NNDC Online Data Service, *http://www.nndc.bnl.gov.*

The Lagrangian of an EFT for nucleons can be described via

$$\mathcal{L} = \mathcal{L}_1 + \mathcal{L}_2 + \mathcal{L}_3 + \cdots \, . \tag{2}$$

By neglecting couplings from weak interactions, the one-body Lagrangian is given by

$$\mathcal{L}_1 = N^\dagger \left(iD_0 + \frac{\boldsymbol{D}^2}{2M_N} - \frac{D_0^2}{2M_N} \right) N \, , \tag{3}$$

where N and M_N are the nucleon field and its mass respectively, D_0 is a covariant derivative, and $\boldsymbol{D}$ and D_0^2 are also the leading relativistic corrections.

The $\mathcal{L}_2$ term of the Lagrangian for two-nucleon interactions, in the ${}^3S_1$ and the ${}^1S_0$ channels as well as ISB corrections, is given by Grießhammer (2005)

$$\begin{aligned}
\mathcal{L}_2 \;=\; & -C_0^{({}^3S_1)} (N^T P_i N)^\dagger (N^T P_i N) \\
& + \frac{C_2^{({}^3S_1)}}{8} \left[(N^T P_i N)^\dagger (N^T (\overleftarrow{\boldsymbol{D}}^2 P_i - 2\overleftarrow{\boldsymbol{D}} \cdot P_i \overrightarrow{\boldsymbol{D}} + P_i \overrightarrow{\boldsymbol{D}}^2) N) + \text{h.c.} \right] \\
& - \frac{C_4^{({}^3S_1)}}{16} \left(N^T \left[P_i \overrightarrow{\boldsymbol{D}}^2 + \overleftarrow{\boldsymbol{D}}^2 P_i - 2\overleftarrow{\boldsymbol{D}} P_i \overrightarrow{\boldsymbol{D}} \right] N \right)^\dagger \left(N^T \left[P_i \overrightarrow{\boldsymbol{D}}^2 + \overleftarrow{\boldsymbol{D}}^2 P_i - 2\overleftarrow{\boldsymbol{D}} P_i \overrightarrow{\boldsymbol{D}} \right] N \right) \\
& - C_0^{({}^1S_0,i)} (N^T \overline{P}_i N)^\dagger (N^T \overline{P}_i N) \\
& + \frac{C_2^{({}^1S_0,i)}}{8} \left[(N^T \overline{P}_i N)^\dagger (N^T (\overleftarrow{\boldsymbol{D}}^2 \overline{P}_i - 2\overleftarrow{\boldsymbol{D}} \cdot \overline{P}_i \overrightarrow{\boldsymbol{D}} + \overline{P}_i \overrightarrow{\boldsymbol{D}}^2) N) + \text{h.c.} \right] \\
& - \frac{C_4^{({}^1S_0,i)}}{16} \left(N^T \left[\overline{P}_i \overrightarrow{\boldsymbol{D}}^2 + \overleftarrow{\boldsymbol{D}}^2 \overline{P}_i - 2\overleftarrow{\boldsymbol{D}} \overline{P}_i \overrightarrow{\boldsymbol{D}} \right] N \right)^\dagger \\
& \left(N^T \left[\overline{P}_i \overrightarrow{\boldsymbol{D}}^2 + \overleftarrow{\boldsymbol{D}}^2 \overline{P}_i - 2\overleftarrow{\boldsymbol{D}} \overline{P}_i \overrightarrow{\boldsymbol{D}} \right] N \right) ,
\end{aligned} \tag{4}$$

where symmetry breaking is incorporated in the description of $C_{2n}^{({}^1S_0,i)} (n = 0, 1, ...)$ coefficients. P_i and $\overline{P}_i$ are

$$\begin{aligned}
P_i \;&\equiv\; \frac{1}{\sqrt{8}} \sigma_2 \sigma_i \tau_2 \, , \quad \text{Tr}\, P_i^\dagger P_j = \frac{1}{2} \delta_{ij} \, , \\
\overline{P}_i \;&\equiv\; \frac{1}{\sqrt{8}} \sigma_2 \tau_2 \tau_i \, , \quad \text{Tr}\, \overline{P}_i^\dagger \overline{P}_j = \frac{1}{2} \delta_{ij} \, .
\end{aligned} \tag{5}$$

For both the ${}^3S_1$ and ${}^1S_0$ channels, the C_{2n} coupling constants have been calculated by fitting to the effective range expansion (Chen & Savage 1999).

The $\mathcal{L}_3$ term in the Lagrangian for three-nucleon forces is (Bedaque et al. 1999)

$$\begin{aligned}
\mathcal{L}_3 \;=\; & -\frac{2MH(\Lambda)}{\Lambda^2} \left(\frac{g_T^4}{4\Delta_T^2} (N^T \tau_2 \sigma_k \sigma_2 N)^\dagger (N^\dagger \sigma_k \sigma_l N)(N^T \tau_2 \sigma_l \sigma_2 N) \right. \\
& + \frac{1}{3} \frac{g_T^2}{2\Delta_T} \frac{g_S^2}{2\Delta_S} \left[(N^T \tau_2 \sigma_k \sigma_2 N)^\dagger (N^\dagger \sigma_k \tau_l N)(N^T \sigma_2 \tau_l \tau_2 N) + \text{h.c.} \right] \\
& \left. + \frac{g_S^4}{4\Delta_S^2} (N^T \sigma_2 \tau_k \tau_2 N)^\dagger (N^\dagger \tau_k \tau_l N)(N^T \sigma_2 \tau_l \tau_2 N) \right) ,
\end{aligned} \tag{6}$$

where the indices T and S denote a field $\boldsymbol{T}$ with spin (isospin) 1 (0) and a field $\boldsymbol{S}$ with spin (isospin) 0 (1), representing two nucleons interacting in the ${}^3S_1$ channel (the deuteron) and the ${}^1S_0$ channel, respectively. The Δ_T (or Δ_S) is the dibaryon field (Bedaque et al. 1999). The Lorentz-invariant Lagrange density that describes the LO interactions has the form (Chen & Savage 1999)

$$\mathcal{L} = d_j^\dagger \left[iD_0 + \frac{\boldsymbol{D}^2}{2M_d} - \frac{D_0^2}{2M_d} \right] d_j + \dots \ . \tag{7}$$

Gauging the above Lagrangian and including the leading relativistic corrections in a direct calculation give

$$\mathcal{L} = d_j^\dagger \left[i(\partial_0 + ieA_0) + (\nabla - ie\boldsymbol{A})^2 \left(\frac{1}{4M_N} + \frac{\gamma^2}{8M_N^3} \right) - (\partial_0 + ieA_0)^2 \left(\frac{1}{4M_N} \right) \right] d_j + \dots \tag{8}$$

One recovers the correct matrix elements of $J^\mu_{\rm em}$, in each order, to reproduce the couplings induced by Equation (7).

The capture amplitude has to be projected on electric and magnetic multipoles that are shown by $E_l(^{2S+1}L_J)$ and $M_l(^{2S+1}L_J)$ respectively, where l is the total angular momentum of the photon, $l \geq 1$, and J, L and S are the total angular momentum, the orbital angular momentum and the spin of the two-nucleons, respectively. The amplitude elements are also constructed with the dibaryon polarization vector $\boldsymbol{\eta}$ and electric or magnetic multipole transition (de Téramond & Gabioud 1987):

$$\begin{array}{ll} E_1 & \epsilon_i = E_i \ , \\ M_1 & (\hat{k} \times \hat{\epsilon})_i = M_i \ , \\ E_2 & \epsilon_i \hat{k}_j + \epsilon_j \hat{k}_i = E_{ij} \ , \dots \end{array} \tag{9}$$

where $\boldsymbol{\epsilon}$ is the photon polarization. To this approximation, the electric and magnetic dipole and electric transition amplitudes are given by (Sadeghi et al. 2006)

$$\begin{aligned} \chi_{E_1} &= \chi^\dagger \{ E_1(^1S_0) \boldsymbol{\epsilon} \cdot \boldsymbol{\eta} + E_1(^1D_2) \epsilon_i \eta_j \mathcal{R}_{ij} \} \chi^c \ , \\ \chi_{M_1} &= \chi^\dagger \{ M_1(^3P_0) i(\boldsymbol{\sigma} \cdot \hat{p}) \boldsymbol{\eta} \cdot (\hat{k} \times \hat{\epsilon}) \\ &\quad + M_1(^3P_1) i(\boldsymbol{\sigma} \times \hat{p}) \cdot [\boldsymbol{\eta} \times (\hat{k} \times \hat{\epsilon})] + M_1(^3P_2) i \epsilon_{ijk} U_{km} \eta_m \hat{k}_i \epsilon_j \} \chi^c \ , \end{aligned} \tag{10}$$

with $x^c = i\sigma_2 x^*$ and $U_{ij} = 3/2(\sigma_i \hat{p}_j + \sigma_j \hat{p}_i) - (\boldsymbol{\sigma} \cdot \hat{p}) \delta_{ij}$.

The contribution of the electric transition for very low-energies is very small and can be ignored. At thermal energies the nd radiative capture only proceeds through the S-wave and magnetic dipole transition. The Lagrange density, involving fields for calculating the M_1 amplitude, is described by (Beane & Savage 2001; Sadeghi & Bayegan 2005)

$$\mathcal{L}_B = \frac{e}{2M_N} N^\dagger (k_0 + k_1 \tau^3) \boldsymbol{\sigma} \cdot \boldsymbol{B} N + e \frac{L_1}{M_N \sqrt{r^{(^1S_0)} r^{(^3S_1)}}} {d_t^j}^\dagger d_{s3} B_j + \text{h.c.} \ , \tag{11}$$

where d_t is the $^3S_1$ dibaryon and d_s is the $^1S_0$ dibaryon. $k_0 = 1/2(k_p + k_n) = 0.4399$ and $k_1 = 1/2(k_p + k_n) = 2.35294$ are also the isoscalar and isovector nucleon magnetic moment in nuclear magnetons, respectively. The L_1 coefficient can be determined phenomenologically (Chen & Savage 1999).

The cross section for the nd $\to$ ^{3}Hγ process at very low-energy is described by (Sadeghi & Bayegan 2005)

$$\sigma = \frac{2}{9} \frac{\alpha}{v_{\rm rel}} \frac{p^3}{4M_N^2} \sum_{iLSJ} [|\widetilde{\chi}_i^{LSJ}|^2] \ , \qquad \widetilde{\chi}_i^{LSJ} = \frac{\sqrt{6\pi}}{p\mu_N} \sqrt{4\pi} \chi_i^{LSJ} \ , \tag{12}$$

where χ is electric or magnetic transitions. μ_N and p are the nuclear magneton and momentum of the incident neutron in the center of mass, respectively.

The solution of the integral equation that describes nd scattering has been discussed before (Bedaque et al. 2000; Grießhammer 2004; Sadeghi & Bayegan 2005). Here we only present the results. The integral is solved numerically for the $^2S_{1/2}$-channel. As long-distance phenomena, the results must be stabilized by introducing a three-body force which absorbs all dependence on the cut-off as $\Lambda \to \infty$ (Bedaque et al. 1999, 2000, 2003; Grießhammer 2004)

$$\mathcal{H}(E;\Lambda) = \frac{2H_0(\Lambda)}{\Lambda^2} + \frac{2H_2(\Lambda)}{\Lambda^4}\,(ME+\gamma_t^2) + \dots\ . \tag{13}$$

For calculation in an isospin symmetric case, this process can be described by an amplitude for scattering into states with $^3S_1$ and $^1S_0$ dibaryons. nd scattering amplitude including the three-body forces is diagramatically shown in Figure 1. In the calculation, two $t_s(d_t+N \to d_s+N)$ and $t_t(d_t+N \to d_t+N)$ amplitudes get mixed (Bedaque et al. 2003):

$$\begin{aligned}
t_s(p,k) \;&= \tfrac{1}{4}\left[3\mathcal{K}(p,k)+2\mathcal{H}(E,\Lambda)\right] \;+\frac{1}{2\pi}\int_0^\Lambda \mathrm{d}q\, q^2 \left[\mathcal{D}_s(q)\left[\mathcal{K}(p,q)+2\mathcal{H}(E,\Lambda)\right] t_s(q)\right.\\
&\qquad \left.+\mathcal{D}_t(q)\left[3\mathcal{K}(p,q)+2\mathcal{H}(E,\Lambda)\right] t_t(q)\right]\ ,\\
t_t(p,k) \;&= \tfrac{1}{4}\left[\mathcal{K}(p,k)+2\mathcal{H}(E,\Lambda)\right] + \frac{1}{2\pi}\int_0^\Lambda \mathrm{d}q\, q^2 \left[\mathcal{D}_t(q)\left[\mathcal{K}(p,q)+2\mathcal{H}(E,\Lambda)\right] t_t(q)\right.\\
&\qquad \left.+\mathcal{D}_s(q)\left[3\mathcal{K}(p,q)+2\mathcal{H}(E,\Lambda)\right] t_s(q)\right]\ ,
\end{aligned} \tag{14}$$

where $\mathcal{D}_{s,t}(q) = \mathcal{D}_{s,t}(E-\frac{q^2}{2M},q)$ is the propagator of dibaryons, for more details see Sadeghi et al. (2006). The amplitudes satisfy the coupled integral equations in Equation (14). The kernels of these equations consist of two terms describing one-nucleon exchange, which provides a long-range force between the dibaryon and the third nucleon, and the three-body contact interaction. When isospin symmetry is broken, we must introduce separate amplitudes for nd scattering into states with $^1S_0$ neutron-neutron and neutron-proton dibaryons, respectively. These satisfy the corresponding set of equations that arise when we allow for ISB effects in the nd system. We notice that the hierarchy of ISB effects observed in the two nucleon system, i.e. charge independent breaking forces are stronger than charge symmetry breaking forces, is not valid for three nucleon forces in the many nucleon system.

The diagrams in Figure 2 denote the photon interaction with nucleon, dibarions and three-body force vertices. We have presented a detailed schematic of these diagrams in nd radiative capture for ($20 \le E \le 200$ KeV) up to N^{2}LO (Sadeghi & Bayegan 2005). For very low energy relevant to big bang nucleosynthesis (BBN), a contribution to the diagram that directly describes the photo-interaction with an exchanged nucleon (third diagram in the sequence) has been neglected. The last diagram of the sequence drawn in Figure 2 shows the insertion of a photon to H_2 vertices and should be calculated when E_2 in higher energies are considered. For calculation of the M_1 transition, first we solve the Faddeev equation for nd scattering and the triton to some order, then we take the calculated Faddeev amplitudes and sandwich it by the photon-interactions with nucleons, when the photon kernel is expanded to the same order; for more details see Sadeghi & Bayegan (2005); Sadeghi et al. (2006).

For the doublet channel, the cross section is determined by $t_t(k,k)$ (the on-shell amplitude), multiplied by the wavefunction renormalization,

$$T(k) = Zt_t(k,k) = \frac{3\pi}{M}\frac{1}{k\cot\delta - \mathrm{i}k}\ , \qquad Z = \frac{8\pi\gamma}{M}\left(1+\gamma\rho+(\gamma\rho)^2+\dots\right). \tag{15}$$

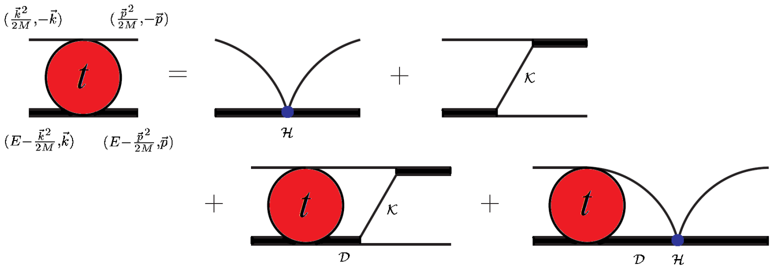

Fig. 1 The Faddeev equation for the nd amplitude. The thick solid line is a propagator of the two intermediate auxiliary fields D_s and D_t, denoted by $\mathcal{D}$; $\mathcal{K}$ is the propagator of the exchanged nucleon; $\mathcal{H}$ is the three-body force.

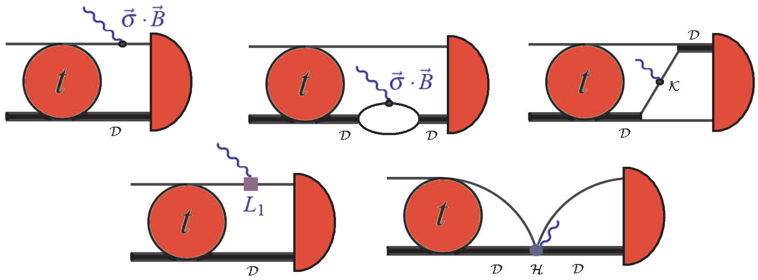

Fig. 2 Diagrams for photon-interaction to the Faddeev equation up to N^{2}LO. The thick lines correspond to either $^1S_0$ or $^3S_1$ dibaryons, while the thin lines represent nucleons. The wavy line shows a photon. The solid circles correspond to an insertion of the single nucleon $\sigma{\cdot}B$ operator. The solid square in the fourth diagram in the sequence denotes the insertion of a four-nucleon-magnetic-photon operator described by a coupling between the $^1S_0$-dibaryon and the $^3S_1$-dibaryon and a magnetic photon. The photon is minimally coupled. The solid circle in the fifth diagram also denotes the insertion of a photon to H_2: three-body force. The remaining notation is the same as in Fig. 1.

The renormalization of Equation (14) is better understood after introducing the variables $t_+ = t_s + t_t$, $t_- = t_s - t_t$, $\mathcal{D}_+ = (\mathcal{D}_s + \mathcal{D}_t)/2$ and $\mathcal{D}_- = (\mathcal{D}_s - \mathcal{D}_t)/2$, in terms of which Equation (14) reads

$$\begin{pmatrix} t_+ \\ t_- \end{pmatrix}(p,k) = \begin{pmatrix} \mathcal{K}(p,k) + \mathcal{H}(E,\Lambda) \\ \frac{1}{2}\mathcal{K}(p,k) \end{pmatrix} + \frac{2}{\pi}\int_0^\Lambda \mathrm{d}q\, q^2$$

$$\begin{pmatrix} \mathcal{D}_+(q)\,[\mathcal{K}(p,q) + \mathcal{H}(E,\Lambda)] & \mathcal{D}_-(q)\,[\mathcal{K}(p,q) + \mathcal{H}(E,\Lambda)] \\ -\frac{1}{4}\mathcal{D}_-(q)\mathcal{K}(p,q) & -\frac{1}{4}\mathcal{D}_+(q)\mathcal{K}(p,q) \end{pmatrix} \begin{pmatrix} t_+ \\ t_- \end{pmatrix}(q,k)\,. \qquad (16)$$

Thus, the arguments given for the renormalization in the bosonic case applies with only minor changes for the $^2S_{\frac{1}{2}}$ channel (Bedaque et al. 2003). The wavefunction renormalization factors are computed from the two-body dibaryon-nucleon bubble, which is explicitly Lorentz invariant (up to the order one computes). To complete the NLO calculation, the wavefunction renormalization constant Z is found from

$$\frac{1}{Z} = \frac{1}{Z_0 + Z_1} \simeq \frac{1}{Z_0} - \frac{Z_1}{Z_0^2} = \frac{1}{Z_0} - i\,\frac{\partial}{\partial p_0}\, i\mathcal{I}_d(p_0, \boldsymbol{p})\Big|_{p_0=E=-E_B} \qquad (17)$$

and thus $Z_1 = Z_0^2$. The NLO amplitude in the quartet channel is therefore given by

$$\begin{aligned} T(k) &= Z\,t(k,k) \simeq (Z_0 + Z_1)(t_0(k,k) + t_1(k,k)) \\ &\simeq T_0(k) + Z_0 t_1(k,k) + Z_1 t_0(k,k) = T_0(k) + T_1(k)\,. \end{aligned} \qquad (18)$$

The phase shift for each partial wave is extracted by expanding both sides of the relation

$$T(k) \simeq T_0(k) + T_1(k)\,. \qquad (19)$$

3 RESULTS AND DISCUSSION

The Faddeev integral equation has been numerically solved up to N^{2}LO with different masses for a neutron and a proton. The parameters we used are as follows: $\hbar c = 197.327$ MeV fm, proton mass = 938.272 MeV, neutron mass = 939.566 MeV, mass difference = 1.293 MeV; for the NN triplet channel a deuteron binding energy (momentum) of $B = 2.225$ MeV ($\gamma_d = 45.7066$ MeV), a residue of $Z_d = 1.690(3)$, effective range $r_{0t} = 2.73$ fm; for the NN singlet channel an $^1S_0$ scattering length of $a_t = -23.714$ fm, $L_1 \sim -4.5$ by fixing its leading non-vanishing order by the thermal cross section and nuclear magneton $\mu_N = 5.050\times10^{-27}JT^{-1}$; for more details see Sadeghi & Bayegan (2005); Sadeghi et al. (2006).

The cut-off was varied between 150 and 500 MeV. The results are shown in Table 1. The error due to varying the cut-off is very small and steadily decreases by increasing the order of the calculation.

Table 1 Comparison between previous results and results without (with) isospin violation at each order. Results for varying the cut-off of the cross section up to N^{2}LO are shown between $\Lambda = 150$ MeV and $\Lambda = 500$ MeV.

E (10^{-8} MeV)	LO (LO(isospin))	NLO (NLO(isospin))	N^{2}LO (N^{2}LO(isospin))
1	0.0006 (0.0004)	0.00005 (0.00004)	0.0000002 (0.0000002)
2	0.0010 (0009)	0.00040 (0.00032)	0.0000005 (0.0000004)
2.65	0.0012 (0.0010)	0.00060 (0.00046)	0.0000090 (0.0000069)
3	0.0014 (0.0011)	0.00084 (0.00067)	0.0000150 (0.0000134)
10	0.0020 (0.0015)	0.00131 (0.00106)	0.0000600 (0.0000453)

The cross section for nd radiative capture as a function of the center-of-mass energy up to N^{2}LO is shown in Figure 3. We also show a single point that represents the available experimental results for this cross section at 0.025 eV (Jurney et al. 1982).

We compare our results with calculations from the other potential model in Table 2. It shows a comparison between results of different models that depend on modern potentials and those that are independent of EFT up to N^{2}LO as well as experimental data. Recent calculations by Viviani et al. (Viviani et al. 1996; Marcucci et al. 1998), with (without) considerations of gauge invariance, are within 10% (15%) of the measured values and these show sensitivity to short-range physics. Song et al. (2009) reported values for the nd radiative capture cross section, about 6% smaller than the measurement, with a larger sensitivity ($\sim 15\%$) to the cut-off variation. They obtained model independent predictions for the thermal capture cross section σ = 0.490±0.008 mb and photon polarization parameter R_c = 0.462±0.03. We have noted the differences between the N^{3}LO M_1 operators used by these authors (their reliance on resonance saturation to constrain the low-energy constants included

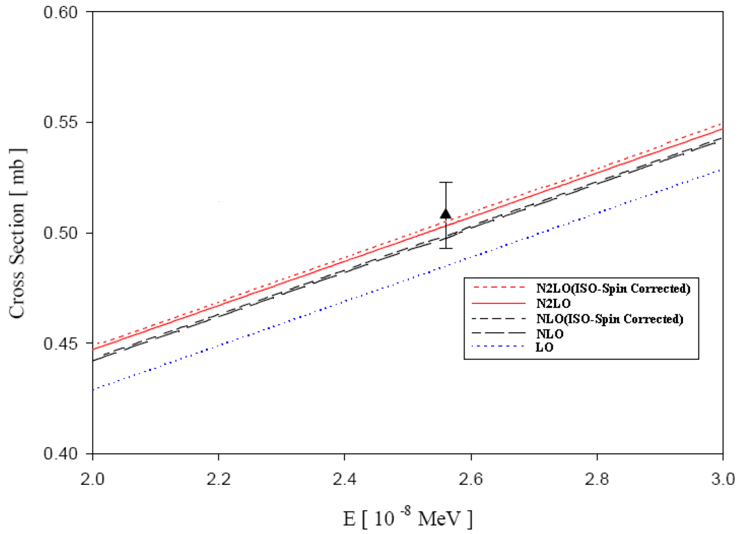

Fig. 3 The cross section for neutron radiative capture by a deuteron as function of the center-of-mass kinetic energy E in MeV. The red dashed line and the red solid line correspond to cross sections of N^2LO with and without isospin correction, respectively. The black short dashed line and black long dashed line correspond to cross sections of NLO with and without isospin correction, respectively. The blue dotted line corresponds to the cross section of the LO case (*color online*). The single point shows experimental results for this cross section at 0.025 eV.

Table 2 Comparison between different theoretical results for neutron radiative capture by a deuteron at thermal energies (0.0253 eV). The bottom rows show our EFT result with and without correction of isospin violation. Errors are estimated in comparison with experimental data.

Theory	σ (mb)	Error
AV14/VIII(IA+MI+MD+Δ_{PT}) (Viviani et al. 1996)	0.658	29%
AV18/IX(IA+MI+MD+Δ_{PT}) (Viviani et al. 1996)	0.631	24%
AV14/VIII(IA+MI+MD+Δ) (Viviani et al. 1996)	0.600	18%
AV18/IX(IA+MI+MD+Δ) (Viviani et al. 1996)	0.578	14%
AV18/IX(gauge inv.) (Marcucci et al. 1998)	0.523	3%
AV18/IX(gauge inv.+3N-Current) (Marcucci et al. 1998)	0.556	10%
HBχPT(N^3LO) (Song et al. 2009)	0.490	3%
EFT(LO) (Sadeghi et al. 2006)	0.485	5%
EFT(LO)+isospin Correction	0.485	5%
EFT(NLO) (Sadeghi et al. 2006)	0.496	3%
EFT(NLO)+isospin Correction	0.497	3%
EFT(N^2LO) (Sadeghi et al. 2006)	0.503	0.9%
EFT(N^2LO)+isospin Correction	0.505	0.5%
Experiment (Jurney et al. 1982)	0.508	

in magnetic moments) and those in our work. The predicted nd radiative capture cross section by Girlanda et al. (2010) is also in good agreement with our data, but exhibit a significant dependence on the input Hamiltonian. Their results are found to be, at least for the case of nd radiative capture, within 4% of the experimental data (Jurney et al. 1982).

The results also show that the importance of isospin violation can be estimated to be of higher order. In fact, the splitting between the $^1S_0$ scattering lengths shown by the neutron-neutron ($a_{\rm nn}$)

and neutron-proton ($a_{\rm np}$) cases can be estimated as $(1/a_{\rm nn} - 1/a_{\rm np})/Q$, where Q is the typical momentum in the system. Counting the nucleon mass in this way ensures that all iterations of the potential contribute to the scattering amplitude at leading order $(q/\Lambda)^0$ and thus have to be resumed. The larger relative size of the ISB corrections compared to the two-nucleon sector should be noted. ISB three-nucleon forces are suppressed by Q/Λ compared to the isospin conserving three-nucleon forces, while the suppression factor in the case of two-nucleon forces is $(Q/\Lambda)^2$. The leading ISB corrections to the two-nucleon and three-nucleon forces arise from different sources. In particular, the dominant contribution to the three-nucleon forces is governed by the proton to neutron mass difference, which only gives a subleading ISB correction to the two-nucleon force. The leading ISB three-nucleon contact interaction is of the order $(Q/\Lambda)^6$ and therefore does not need to be included.

4 SUMMARY AND CONCLUSIONS

Calculation of the cross section for nd radiative capture at zero energies, using pionless EFT, provides a unique, model independent and systematic low-energy version of QCD for processes involving momenta below the pion mass. We applied pionless EFT to find numerical results for the M_1 transition by considering isospin violation.

At very low-energies relevant for BBN, $M1$ contributes the dominant term to the calculation. Three-nucleon forces are also considered for accurate calculation and are needed up to order N^{2}LO for results that are independent of the cut-off. Hence, cross section is completely determined to be $\sigma_{\rm tot} = [0.485({\rm LO}) + 0.012({\rm NLO}) + 0.008({\rm N^2LO})] = [0.505 \pm 0.003]$ mb, by considering isospin effects in higher order calculations. The uncertainty in the calculated cross section at very low energy (0.0253 eV) is estimated to be less than 1% up to N^{2}LO.

For future calculations, this study should be extended in various directions. A more systematic study of ISB in the processes including two- and three-nucleon systems, based on the formalism developed here, should be pursued. In particular, one should construct the electroweak current operators to the same accuracy and work out the corresponding three-nucleon force.

Acknowledgements This work is supported in part by Arak University.

References

Beane, S. R., & Savage, M. J. 2001, Nuclear Physics A, 694, 511
Bedaque, P. F., Hammer, H.-W., & van Kolck, U. 1999, Physical Review Letters, 82, 463
Bedaque, P. F., Hammer1, H.-W., & van Kolck, U. 2000, Nuclear Physics A, 676, 357
Bedaque, P. F., Rupak, G., Grießhammer, H. W., & Hammer, H.-W. 2003, Nuclear Physics A, 714, 589
Chen, J. W., & Savage, M. J. 1999, Physics Letters B, 464, 1
de Téramond, G. F., & Gabioud, B. 1987, Phys. Rev. C, 36, 691
Epelbaum, E., & Meißner, U.-G. 2005, Phys. Rev. C, 72, 044001
Epelbaum, E., Meissner, U.-G., & Palomar, J. E. 2005, Phys. Rev. C, 71, 024001
Friar, J. L., Gibson, B. F., & Payne, G. L. 1990, Physics Letters B, 251, 11
Friar, J. L., van Kolck, U., Rentmeester, M. C., & Timmermans, R. G. 2004, Phys. Rev. C, 70, 044001
Girlanda, L., Kievsky, A., Marcucci, L. E., et al. 2010, Physical Review Letters, 105, 232502
Grießhammer, H. W. 2004, Nuclear Physics A, 744, 192
Grießhammer, H. W. 2005, Nuclear Physics A, 760, 110
Iqbal, M. J., & Niskanen, J. A. 1988, Phys. Rev. C, 38, 2259
Jurney, E. T., Bendt, P. J., & Browne, J. C. 1982, Phys. Rev. C, 25, 2810
Marciano, W., & Pagels, H. 1978, Phys. Rep., 36, 137
Marcucci, L. E., Riska, D. O., & Schiavilla, R. 1998, Phys. Rev. C, 58, 3069
Sadeghi, H. 2007, Phys. Rev. C, 75, 044002

Sadeghi, H. 2008, Few-Body Systems, 44, 149
Sadeghi, H., & Bayegan, S. 2005, Nuclear Physics A, 753, 291
Sadeghi, H., & Bayegan, S. 2010, Few-Body Systems, 47, 167
Sadeghi, H., Bayegan, S., & Grießhammer, H. W. 2006, Physics Letters B, 643, 263
Song, Y.-H., Lazauskas, R., & Park, T.-S. 2009, Phys. Rev. C, 79, 064002
van Kolck, U., Rentmeester, M. C. M., Friar, J. L., Goldman, T., & de Swart, J. J. 1998, Physical Review Letters, 80, 4386
Viviani, M., Schiavilla, R., & Kievsky, A. 1996, Phys. Rev. C, 54, 534
Walzl, M., Meißner, U.-G., & Epelbaum, E. 2001, Nuclear Physics A, 693, 663